Available online at www.sciencedirect.com
SCIENCE DIRECT®
Biochemical and Biophysical Research Communications 335 (2005) 112–116
BBRC
www.elsevier.com/locate/ybbrc

$L^{565}M$ mutation in HIV-1 glycoprotein 41 stabilizes the coiled-coil structure

Daisuke Yamamoto [a,*], Gui-Mei Li [b], Kazuyoshi Ikuta [b], Toshiyuki Goto [c]

[a] *Biomedical Computation Center, Osaka Medical College, Takatsuki, Osaka 569-8686, Japan*
[b] *Department of Virology, Research Institute for Microbial Diseases, Osaka University, Suita, Osaka 575-0871, Japan*
[c] *School of Health Science, Faculty of Medicine, Kyoto University, Kyoto 606-8507, Japan*

Received 1 July 2005
Available online 28 July 2005

Abstract

N-terminal and C-terminal heptad repeats (NHR and CHR) of HIV type 1 (HIV-1) glycoprotein 41 are known to be regions directly related to cell fusion during virus attack, and their complex core constructs a coiled-coil structure in the fusion process. In our recent studies, MT-4/17-3-6, a strain of HIV-1, showed the strong resistance to peptide fusion inhibitors compared with other strains such as MT-4/LAI, L-2 and CU98-26, and had a distinctive $L^{565}M$ mutation in the central region of NHR. To investigate the relationship between the mutation and resistance, we performed a molecular modeling of the coiled-coil of MT-4/17-3-6 by using energy minimization and molecular dynamics simulation based on the MT-4/LAI X-ray structure. As a result, we found that H^{564} in the NHR was pushed to the outer side by this mutation, and three hydrogen bond bridges of Y^{638}-H^{564}-E^{560}-Q^{650} could be formed, enclosing the coiled-coil. The binding of peptide inhibitors would be disturbed by the structural stabilization of these bridges in MT-4/17-3-6.

Keywords: HIV-1 gp41; Spike protein; Mutation; Cell fusion; Molecular modeling

The ectodomain of human immunodeficiency virus type 1 (HIV-1) glycoprotein 41 (gp41) has been investigated as a part of the spike protein directly related to the cell fusion of virus, and it consists of fusion protein (FP), N-terminal heptad repeats (NHR), interdomain fusion protein (IFP), C-terminal heptad repeats (CHR), and other regions [1]. Studies by electron microscopy [2–4] demonstrated that the spike protein of HIV-1 formed a trimer complex in fusion process. In addition, molecular structure analyses [5–7] revealed that NHR and CHR had similar helical conformations packed in an anti-parallel manner, and that the three pairs of NHR and CHR in a trimer gp41 were arranged tightly in a trimeric coiled-coil. Three NHR regions were coiled in the inner side and the three CHR regions covered the NHR coil on the outer side. This coiled-coil complex could be constructed by conformational changes of glycoprotein 120 interacting with CD4 and CXCR4 coreceptor [8,9]. Formation of the coiled-coil causes the viral envelope to approach the target cell membrane via tight binding, and allows membrane fusion associated with rapid entry of the viron core into the target cell [1,10,11]. Thus, the NHR–CHR interactions are very important for investigating the fusion mechanism of the virus entry process and for designing the inhibitors against the cell fusion.

One complicating fact is that HIV-1 is genetically variable [12]. Among HIV-1 genome, *env* gene has been widely used for the classification by phylogenetic analysis [13]. Based on the sequence of complete viral genomes [14], HIV-1 nucleotide sequences circulating in the world have been divided into three groups: M

* Corresponding author. Fax: +81 72 684 6429.
E-mail address: center@art.osaka-med.ac.jp (D. Yamamoto).

0006-291X/$ - see front matter © 2005 Elsevier Inc. All rights reserved.
doi:10.1016/j.bbrc.2005.07.052

Table 1
Amino acid sequences of the NHR and CHR regions of HIV-1s used in our previous research [23]

HIV-1	Subtype	Amino acid sequence[a]	
		NHR	CHR
		546 579	628 661
MT-4/LAI	B	SGIVQQQNNLLRAIEAQQHLLQLTVWGIKQLQAR	WMEWDREINNYTSLIHSLIEESQNQQEKNEQELL
L-2	B	----------	----------
MT-4/17-3-6	B	-------D----------M----------	--Q-E---D---G--YN------I------KD--
CU98-26	AE	-------S----------	-T--E---S----Q-YDILT------DR--KD--

[a] A dash (-) indicates identity with the corresponding MT-4/LAI amino acid residue.

(major); O (outlier); and N (non-M or O). Within the most prevalent group, M, there are at least eight discrete subtypes (A, B, C, D, F, G, H, and J) and 14 circulating recombinant forms. Different HIV-1 subtypes and recombinant forms are generally associated with different countries and continents [15,16], and the similarities among these subtypes are distributed widely [17,18]. It was also reported that homologous synthetic peptides of the NHR and CHR regions, called N34 and C34, had binding activities to CHR and NHR, respectively [19–21]. Therefore, these synthetic peptides play an important role as experimental tools for studies of cell fusion and its inhibition because of the affinities to gp41.

We have studied the fusion mechanism to identify the important factors for the design of inhibitors, and reported that strain MT-4/17-3-6 [22] from a Japanese patient with acquired immunodeficiency syndrome (AIDS) showed stronger resistance against both N34 and C34 peptides than other strains, MT-4/LAI, L-2, and CU98-26 [23]. In this article, to investigate the basis of the resistance of MT-4/17-3-6, an NHR–CHR complex model was predicted stereo-chemically by molecular modeling with energy minimization and dynamics simulation. We compared it with MT-4/LAI model, especially focusing the central region of the coiled-coil, which was not markedly affected by any other parts of the envelope protein. This central region includes the M^{565} of MT-4/17-3-6, which is mutated distinctively from the L^{565} of MT-4/LAI, L-2 and CU98-26. The amino acid sequences of NHR and CHR of these strains are summarized in Table 1.

Materials and methods

Molecular modeling of MT-4/17-3-6 NHR–CHR complex. The initial model for the MT-4/17-3-6 complex was constructed by using of residue replacements on the coordinate sets 1AIK in Protein Data Bank [5], a NHR–CHR complex X-ray model of MT-4/LAI. Structural optimization was performed for this model by an energy minimization method with an MMFF94 force field [24] considering water molecules within 10 Å around protein atoms. The energy cutoff distance was set at 10 Å and the dielectric constant was distance dependent based on the value of 1.0 for the protein atoms and 80.0 for the solvent atoms. The 1AIK X-ray model of MT-4/LAI was optimized for comparison with the MT-4/17-3-6 model by the same method.

100 ps molecular dynamics simulation was performed for each optimized model with the water molecules at 300 K by using a 0.002 ps time step, the MMFF94 force field and NVT method (number of particles, volume, and temperature were fixed) [25–27]. Before these equilibrium iterations, 1ps heating iterations were employed to consider the stable equilibration. The potential energy of each total molecular system after the 100 ps simulation was -5.85×10^4 kcal/mol and -5.67×10^4 kcal/mol, including 3233 and 3252 water molecules for MT-4/17-3-6 and MT-4/LAI, respectively. Hydrogen bond analyses were based on 100 conformations sampled every 0.5 ps during the equilibrium iterations from 50 to 100 ps, in which the potential energy seemed to settle down clearly.

All operations and calculations were performed using a graphical package for molecular structure analyses, Molecular Operating Environment (CCG, http://www.ccg.com/).

Results and discussion

A possible structure of the MT-4/17-3-6 NHR–CHR complex predicted from energy minimization is shown in Fig. 1A. We found three sets of hydrogen bond bridges which seemed to fix the complex effectively. The bridge consisted of three hydrogen bonds of $Y^{638}O^{\eta}$–$H^{564}N^{\delta1}$, $H^{564}N^{\varepsilon2}$–$E^{560}O^{\delta1}$ and $E^{560}O^{\delta2}$–$Q^{650}N^{\varepsilon2}$, and three of the bridges enclosed the complex on its surface. The alignment of functional groups in the bridge was seemed to be similar to the charge relay system of serine protease active sites. In the structure of the MT-4/LAI NHR–CHR complex, shown in Fig. 1B, only $E^{560}O^{\delta2}$–$Q^{650}N^{\varepsilon2}$ was formed and $Y^{638}O^{\eta}$–$H^{564}N^{\delta1}$ and $H^{564}N^{\varepsilon2}$–$E^{560}O^{\delta1}$ were not formed. Especially, the phenyl ring of Y^{638} and the imidazole ring of H^{564} existed side by side, but O^{η} and $N^{\delta1}$ or $N^{\varepsilon2}$ were not placed where they could form a hydrogen bond. The sidechain of H^{564} in the MT-4/17-3-6 complex shifted slightly to the outer side of the complex compared with the MT-4/LAI complex, and it was thought that the formation of hydrogen bonds of $Y^{638}O^{\eta}$–$H^{564}N^{\delta1}$ and $H^{564}N^{\varepsilon2}$–$E^{560}O^{\delta1}$ was enable by this shift. The total interaction energy between NHR and CHR was -4.52×10^2 kcal/mol in MT-4/17-3-6 and -4.05×10^2 kcal/mol in MT-4/LAI; thus, the NHR and CHR of MT-4/17-3-6 were combined more strongly than these of MT-4/LAI.

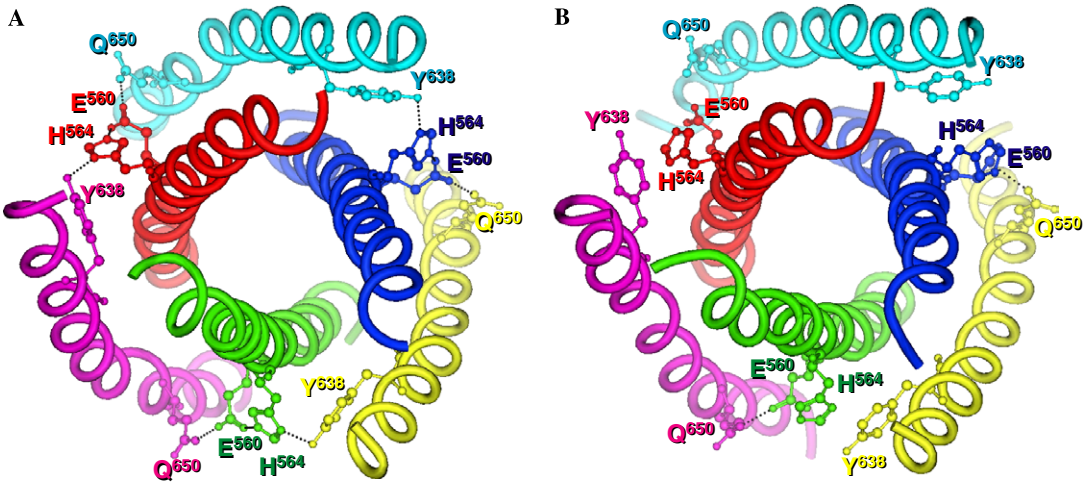

Fig. 1. Optimized models of MT-4/17-3-6 and MT-4/LAI NHR–CHR complex. The optimized structures of the NHR–CHR regions of MT-4/17-3-6 and MT-4/LAI are shown by tube models with ball and stick models of Y^{638}, H^{564}, E^{560}, and Q^{650} in A and B respectively. The helical structures of the NHR core coiled-coil are colored by red, blue and green, and the helical structures of CHR are colored by purple, light blue and yellow. Possible hydrogen bonds are shown by black dotted lines.

The statistical analyses of the formation of these hydrogen bonds during the later iterations of the molecular dynamics simulations are summarized in Table 2, and a superimposed stereo view of the most stable structure in the simulations is shown in Fig. 2. In the MT-4/17-3-6 complex, hydrogen bonds were formed in the conformation with probabilities of 82.3% and 59.7% for $Y^{638}O^{\eta}$–$H^{564}N^{\delta1}$ and $H^{564}N^{\varepsilon2}$–$E^{560}O^{\delta1}$ respectively, which are very high probabilities compared with these for MT-4/LAI. Just beside H^{564}, the $L^{565}M$ mutation was found in MT-4/17-3-6 compared with MT-4/LAI. In the MT-4/LAI complex, as shown by dark blue and green sticks in Fig. 2, the L^{565} sidechain contacted CHR sidechains of I^{635} and I^{642} by hydrophobic interaction, and this interaction was fixed tightly by the existence of a hydrogen bond between Q^{567} and T^{639}. On the other hand, in the MT-4/17-3-6 complex, as shown by orange and yellow sticks, a longer hydrophobic sidechain of M^{565} existed instead of the shorter sidechain of leucine. Two isoleucines, glutamine and threonine in the MT-4/17-3-6 complex remained at the same positions in the MT-4/LAI complex and fixed the sidechain of methionine. In addition, the I^{635} residue, especially its sidechain, was close to the sidechain of M^{565} because of loss of the branched structure in the sidechain L^{565}.

We found that H^{564} in the NHR was pushed to the outer side in the MT-4/17-3-6 complex, and three hydrogen bond bridges of Y^{638}–H^{564}–E^{560}–Q^{650} could be formed and seen to enclose the coiled-coil. As shown in detail in Fig. 2, the structural difference from the MT-4/LAI complex in this region was that the M^{565} mainchain and the H^{564} of NHR were pushed to the outer side (from dark blue to orange) and the neighboring Y^{638} and T^{639} of CHR were shifted to the opposite direction (from green to yellow). As a result, the imidazole ring of H^{564} in the MT-4/17-3-6 complex was placed in the position and direction where it could be stabilized by hydrogen bonds with both Y^{638} in the CHR region and E^{560} in the same NHR region.

We tentatively optimized another virtual model with mutation of only $L^{565}M$ from MT-4/LAI, and also found similar Y^{638}–H^{564} hydrogen bonds as in the MT-4/17-3-6 model (data not shown). As shown in Table 1, $E^{630}Q$, $S^{641}G$, and $N^{651}I$ mutations were found distinctively in the CHR region of MT-4/17-3-6, but all of these residues were placed on the outer side, which had no direct interaction with the inner NHR coils. $S^{641}G$ and $N^{651}I$ were adjacent to Y^{638} and Q^{650}. It seemed that these mutations might contribute to the formation of hydrogen bond bridges by increasing the

Table 2
Probability of hydrogen bond formation during the molecular dynamics simulation

Models	Probability of hydrogen bond formation (%)[a]		
	$Y^{638}O^{\eta}$–$H^{564}N^{\delta1}$	$H^{564}N^{\varepsilon2}$–$E^{560}O^{\delta1}$	$E^{560}O^{\delta2}$–$Q^{650}N^{\varepsilon2}$
MT-4/17-3-6	82.3	59.7	74.3
MT-4/LAI	1.0	0.3	76.7

[a] Hydrogen bond analyses were based on 100 conformations sampled every 0.5 ps during the equilibrium iterations from 50 to 100 ps. The criteria for hydrogen bond formation were as following; bond length of N–O < 3.6 Å and bond angle of N–H–O > 110°.

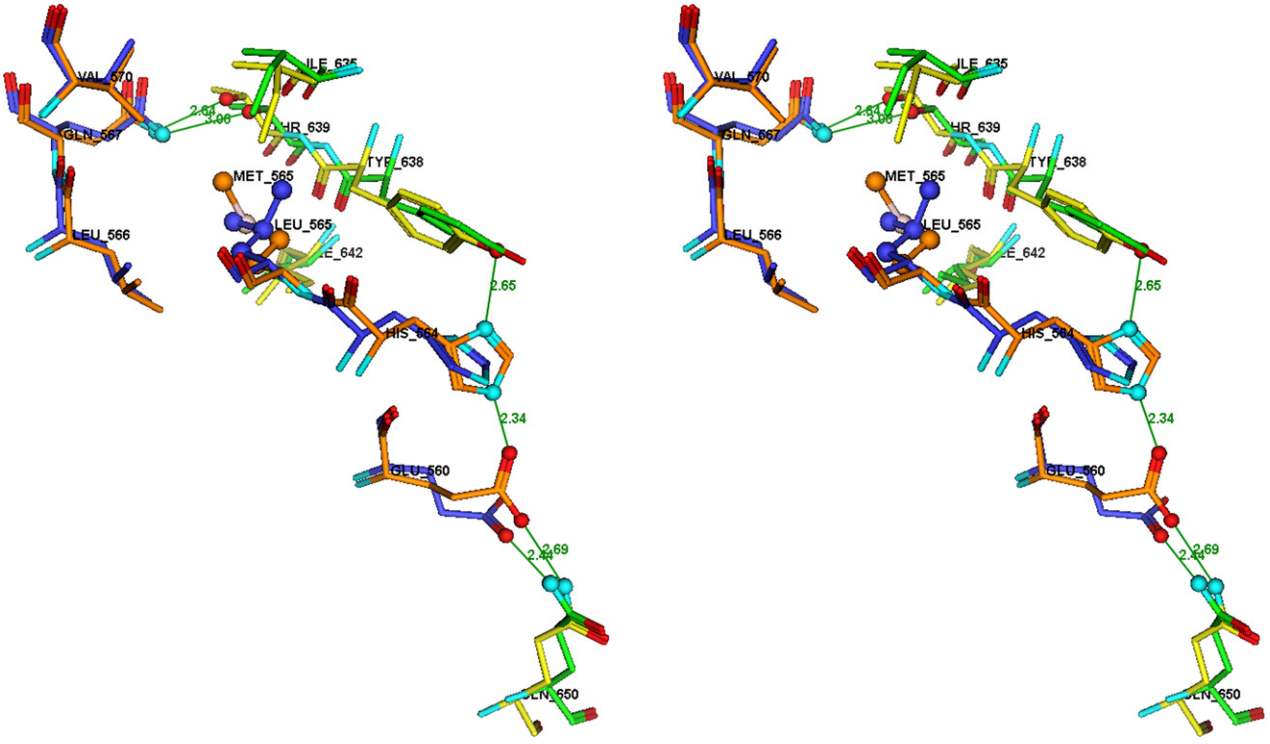

Fig. 2. A superimposed stereo view of the molecular models of MT-4/17-3-6 and MT-4/LAI. The most stable structures in our molecular dynamics simulations of MT-4/17-3-6 and MT-4/LAI were superimposed by a fitting of all mainchain atoms, and only parts related to the hydrogen bond bridges of MT-4/17-3-6 are shown. The NHR and CHR regions of MT-4/17-3-6 are shown by orange and yellow sticks, and these of MT-4/LAI by dark blue and green sticks, respectively. Oxygen, nitrogen, and sulfur atoms are colored by red, light blue, and white. Each hydrogen bond and its length is shown by a green line and numerical value, and the atoms involved in these hydrogen bonds and sidechains of the 565th residues are shown by a ball and stick model.

flexibilities of the neighboring mainchain of Y^{638} and decreasing the hydrogen bonding to the Q^{650} sidechain via water molecules, respectively.

Therefore, it was thought that the $L^{565}M$ mutation would be a major factor affecting the coiled-coil stabilization by these bridges, and the binding of peptide fusion inhibitors might be distinctively disturbed by this stabilization in MT-4/17-3-6. The parallel stacking of two rings of H^{564} and Y^{638} was also found in the X-ray structure [7], but no hydrogen bond between these sidechains was shown in the structure, because the two rings were placed too closely, as was also true in the MT-4/LAI model. We think that the hydrogen bond between H^{564} and Y^{638} fixes the sidechain of H^{564} in the position that makes it easy to form the next hydrogen bond with E^{560}, and that the positional relationship of the two rings is very important for the total formation of the hydrogen bond bridges shown in the model for MT-4/17-3-6.

Coiled-coil trimeric structures are commonly found in the spike proteins of not only HIV but also other corona viruses, including influenza virus, Ebola virus, and SARS virus [28]. In these coiled-coil structures, it seemed that HIV had the most tightly combined complex of NHR and CHR, and therefore the mode of interaction between NHR and CHR of HIV may be most effective for the trimeric formation at the time of virus attack. We found in our previous research that the differences of gp41 resistance to peptide fusion inhibitors were larger for intra-subtype comparisons, such as MT-4/LAI and MT-4/17-3-6, than for inter-subtype comparisons, such as MT-4/LAI and CU98-26 (subtypes are shown in Table 1) [23]. These large intra-subtype differences can be explained by our model, which showed that the $L^{565}M$ mutation could stabilize the coiled-coil without affecting the structure of the protein widely. We previously reported that the resistance to peptide fusion inhibitors differed markedly between MT-4/LAI and L-2 in spite of the fact that they had the same sequences of NHR and CHR (Table 1). It is not thought that all of the differences between these virus strains could be explained in here clearly, because the interactions between the NHR–CHR complex and the other regions of the spike protein were not considered in our analyses. However, by the focusing on the $L^{565}M$ mutation in the inner and central moiety, which would be not affected by the other regions, we found that this mutation might be an important factor for the resistance of MT-4/17-3-6 to peptide inhibitors with respect to coiled-coil formation and cell fusion.

References

[1] D.C. Chan, P.S. Kim, HIV entry and its inhibition, Cell 93 (1998) 681–684.

[2] H.R. Gelderblom, M. Ozel, G. Pauli, Morphogenesis and morphology of HIV. Structure–function relations, Arch. Virol. 106 (1989) 1–13.

[3] M. Ozel, G. Pauli, H.R. Gelderblom, The organization of the envelope projections on the surface of HIV, Arch. Virol. 100 (1988) 255–266.

[4] T. Goto, M. Nakai, K. Ikuta, The life-cycle of human immunodeficiency virus type 1, Micron 29 (1998) 123–138.

[5] D.C. Chan, D. Fass, J.M. Berger, P.S. Kim, Core structure of gp41 from the HIV envelope glycoprotein, Cell 89 (1997) 263–273.

[6] W. Weissenhorn, A. Dessen, S.C. Harrison, J.J. Skehel, D.C. Wiley, Atomic structure of the ectodomain from HIV-1 gp41, Nature 387 (1997) 426–430.

[7] J. Liu, W. Shu, M.B. Fagan, J.H. Nunberg, M. Lu, Structural and functional analysis of the HIV gp41 core containing an Ile573 to Thr substitution: implications for membrane fusion, Biochemistry 40 (2001) 2797–2807.

[8] P.L. Jones, T. Korte, R. Blumenthal, Conformational changes in cell surface HIV-1 envelope glycoproteins are triggered by cooperation between cell surface CD4 and co-receptors, J. Biol. Chem. 273 (1998) 404–409.

[9] S.A. Gallo, A. Puri, R. Blumenthal, HIV-1 gp41 six-helix bundle formation occurs rapidly after the engagement of gp120 by CXCR4 in the HIV-1 Env-mediated fusion process, Biochemistry 40 (2001) 12231–12236.

[10] Y. He, R. Vassell, M. Zaitseva, N. Nguyen, Z. Yang, Y. Weng, C.D. Weiss, Peptides trap the human immunodeficiency virus type 1 envelope glycoprotein fusion intermediate at two sites, J. Virol. 77 (2003) 1666–1671.

[11] S. Shnaper, K. Sackett, S.A. Gallo, R. Blumenthal, Y. Shai, The C- and the N-terminal regions of glycoprotein 41 ectodomain fuse membranes enriched and not enriched with cholesterol, respectively, J. Biol. Chem. 279 (2004) 18526–18534.

[12] M. Peeters, P.M. Sharp, Genetic diversity of HIV-1: the moving target, Aids 14 (Suppl 3) (2000) S129–S140.

[13] T. Leitner, Genetic subtypes of HIV-1, in: Human Retroviruses and AIDS 1996: A Complilation and Analysis of Niucleic Acid and Amino Acid Sequences G. Myers, B. Korber, B. Foley, K.-T. Jeang, J.W. Mellors, S. Wain-Hobson, (eds.), Los Alamos National Laboratory, Los Alamos, New Mexico, part III (1996) pp. 28-40.

[14] WHO Network for HIV Isolation and Characterization, HIV-1 variation in World Health Organization-sponsored vaccine evaluation sites: genetic screening, sequence analysis, and preliminary biological characterization of selected viral strains, AIDS Res. Hum. Retroviruses 10 (1994) 1327–1343.

[15] S. Osmanov, C. Pattou, N. Walker, B. Schwardlander, J. Esparza, WHOUNAIDS network for HIV isolation and characterization, estimated global distribution and regional spread of HIV-1 genetic subtypes in the year 2000, J. Acquir. Immune. Defic. Syndr. 29 (2002) 184–190.

[16] C.Y. Ou, Y. Takebe, C.C. Luo, M. Kalish, W. Auwanit, C. Bandea, N. de la Torre, J.L. Moore, G. Schochetman, S. Yamasaki, H. Gayle, N. Young, B.G. Weniger, Wide distribution of two subtypes of HIV-1 in Thailand, AIDS Res. Hum. Retroviruses 8 (1992) 1471–1472.

[17] J.M. Coffin, HIV population dynamics in vivo: Implications for genetic variation, pathogenesis and therapy, Science 267 (1995) 483–489.

[18] D.L. Robertson, P.M. Sharp, F.E. McCutchan, B.H. Hahn, Recombination in HIV-1, Nature (London) 374 (1995) 124–126.

[19] S. Jiang, K. Lin, N. Strick, A.R. Neurath, HIV-1 inhibition by a peptide, Nature 365 (1993) 113–113.

[20] C. Wild, T. Oas, C. McDanal, D. Bolognesi, T. Matthews, A synthetic peptide inhibitor of human immunodeficiency virus replication: correlation between solution structure and viral inhibition, Proc. Natl. Acad. Sci. USA 89 (1992) 10537–10541.

[21] C. Wild, D. Shugars, T. Greenwell, C. McDanal, T. Matthews, Peptides corresponding to a predictive alpha-helical domain of human immunodeficiency virus type 1 gp41 are potent inhibitors of virus inhibitors of virus infection, Proc. Natl. Acad. Sci. USA 91 (1994) 9770–9774.

[22] T. Mukai, S. Komoto, T. Kurosu, J.A. Palacios, Y.G. Li, W. Auwanit, M. Tatsumi, K. Ikuta, Construction and characterization of an infectious molecular clone derived from the CRF01_AE primary isolate of HIV type 1, AIDS Res. Hum. Retroviruses 18 (2002) 585–589.

[23] P. Isarangkura N.A., G.M. Li, J. Warachit, Y. Iwabu, S. Tsuji, W. Auwanit, D. Yamamoto, T. Goto, Y. Hayashi, Y. Kiso, K. Ikuta, Different susceptibility of human immunodeficiency virus type 1 to Env gp41-derived synthetic peptides corresponding to the C-terminal heptad repeat regions, Microbes Infect. 7 (2005) 356–364.

[24] T.A. Halgren, Merck molecular force field. I. Basis, form, scope, parameterization, and performance of MMFF94, J. Comput. Chem. 17 (1996) 490–519;
T.A. Halgren, Merck molecular force field. II. MMFF94 van der Waals and electrostatic parameters for intermolecular interactions, J. Comput. Chem. 17 (1996) 520–552;
T.A. Halgren, Merck molecular force field. III. Molecular geometries and vibrational frequencies for MMFF94, J. Comput. Chem. 17 (1996) 553–586;
T.A. Halgren, R.B. Nachbar, Merck molecular force field. IV. conformational energies and geometries for MMFF94, J. Comput. Chem. 17 (1996) 587–615;
T.A. Halgren, Merck molecular force field. V. Extension of MMFF94 using experimental data, additional computational data, and empirical rules, J. Comput. Chem. 17 (1996) 616–641.

[25] H.J.C. Berendsen, J.P.M. Postma, W.F. Van Gunsteren, A. Di Nola, J.R. Haak, Molecular dynamics with coupling to an external bath, J. Chem. Phys. 81 (1984) 3684–3690.

[26] S.D. Bond, J.L. Benedict, B.B. Laird, The nos-poincar method for constant temperature molecular dynamics, J. Comp. Physiol. 151 (1999) 114–134.

[27] J.B. Sturgeon, B.B. Laird, Symplectic Algorithm for Constant Pressure Molecular Dynamics Using a Nos-Poincar Thermostat. University of Kansas Technical Paper (2002).

[28] Y. Xu, Y. Liu, Z. Lou, L. Qin, X. Li, Z. Bai, H. Pang, P. Tien, G.F. Gao, Z. Rao, Structural basis for coronavirus-mediated membrane fusion—crystal structure of mouse hepatitis virus spike protein fusion core, J. Biol. Chem. 279 (2004) 30514–30522.